Selective spectral displacement projection in 3D multifrequency MRE

Temel Kaya Yasar[1], Dieter Klatt[2], Richard L. Magin[2], and Thomas J. Royston[2]

[1]*Department of Mechanical & Industrial Engineering, The University of Illinois at Chicago, Chicago, Illinois, United States,* [2]*Department of Bioengineering, The University of Illinois at Chicago, Chicago, Illinois, United States*

Introduction: In Magnetic Resonance Elastography (MRE), external vibrations are introduced into the target tissue, measured via phase-contrast based MRI and analyzed for determining tissue mechanical properties [1]. As opposed to conventional, monofrequency MRE, where the mechanical behavior of tissue is identified at one specific frequency, multifrequency MRE enables the determination of frequency-independent material parameters [2]. While remarkable insights into the correlation of pathophysiological changes and the mechanical structure of tissue have been gained by multifrequency MRE [3-4], solely out-of-plane displacements were taken into account. However, the acquisition of the 3D displacement field, which is already performed in monofrequency MRE [5-6], exhibits advantages, as the shear wave can be separated from the compression wave [5], and as compressional properties can also be considered [6]. **Problem:** The acquisition of 3D multifrequency MRE data is time-consuming using conventional monofrequency MRE approaches, because each of the three displacement projections has to be determined for each of the spectral components in consecutive steps. Further, the fragmentation into individual experiments potentially gives rise to errors, e.g. due to misalignment of the image slice or due to a varying transmission of mechanical energy from one individual physical vibration state to the other. An alternative to the successive application of monofrequency MRE would be the use of fractional motion encoding schemes [7] in order to simultaneously measure the excited vibration spectrum for each displacement projection resulting in only three individual experiments. However, this procedure implies reduced motion sensitivity that cannot be enhanced by increasing the MEG cycle number. **Objective:** We introduce a new motion-encoding scheme for the acquisition of 3D multifrequency vibrations composed of three frequencies. In the new approach, which we call *selective spectral displacement projection* (SDP)-MRE, MEGs of different frequency are applied simultaneously along the three directions while obeying the filter condition [8]. This enables a reduction in the necessary number of individual temporally-resolved MRE experiments from nine to three with the same motion sensitivity as in conventional MRE.

Theory: Henceforth, the index j=1, 2, 3 corresponds to the read-, phase-, and slice-direction in the scanner system, respectively and to the x-, y- and z-direction in the Cartesian system. No harmonic motion is encoded in the MR signal phase ϕ, if the filter condition [8], which represents the basis for SDP-MRE, holds for the vibration frequency f, the MEG-cycle number N_j and the duration τ_j of one cycle of the MEG-gradient in j-direction: $f = \frac{n}{N_j \tau_j} = \frac{n}{T},\ n \in \mathbb{N}\backslash\{N_j\}$. Of specific note, SDP-MRE implies that the MEG-duration T is equal to $T=N_j\tau_j$ for all projections j. In SDP-MRE, a vibration spectrum composed of three frequencies is excited and the vibration frequencies are chosen for matching the frequencies of the MEG-projections $1/\tau_j$. The filter condition reveals that the base frequency f_b defined as the reciprocal of T does not contribute to the accumulation of ϕ. Further, all multiples of f_b are filtered out with the exception of $1/\tau_j$. Thus, with regard to one motion component, only the vibration corresponding to the frequency of the respective MEG-component contributes to ϕ. Consequently, the total MR phase ϕ is represented by a sum of phase portions ϕ_j, each corresponding to a distinct spatial projection and vibration frequency.

Methods: SDP-MRE was applied to a phantom consisting of an agarose bead (0.7%) embedded in agarose gel (1.1%). The basic MRE setup used in the experimental 11.7T Bruker vertical MRI system has been described elsewhere [9]. The sample bin (= 9 mm) was positioned inside a 10 mm birdcage RF coil and was driven by a piezostack actuator attached to an inertial ground mass. We used a gradient-echo sequence upgraded with motion encoding gradients for data acquisition in an axial slice with the following sequence parameters: TR=500 ms; TE=7.94 ms; flip angle=30°; FOV=10x10 mm^2; matrix size=128^2; slice thickness=0.25 mm; MEG amplitude=80 G/cm. As shown in fig. 1, the excitation signal was a superposition of 5 kHz-, 6 kHz- and 7 kHz-sinusoidal waveforms. We exploited the filter condition by choosing an MEG gradient cycle number of 15, 18 and 21, and an MEG frequency of 5 kHz, 6 kHz and 7 kHz for the read-, phase- and slice-direction, respectively. The trigger was shifted 16 times over the 1 ms-interval to acquire $\phi(s)$ as a function of the start time s of the MEG. For frequency decomposition, the Fourier-transformation of $\phi(s)$ was calculated and the respective components were scaled to displacements. A 2D local frequency estimation (LFE) algorithm [10] was applied to the images and the resulting wavelength was spatially averaged over the bead. For comparison of SDP-MRE and conventional MRE, the same experiment was repeated three times with the only difference being that only one of the three MEGs shown in fig. 1 was applied in each of the repetitive experiments.

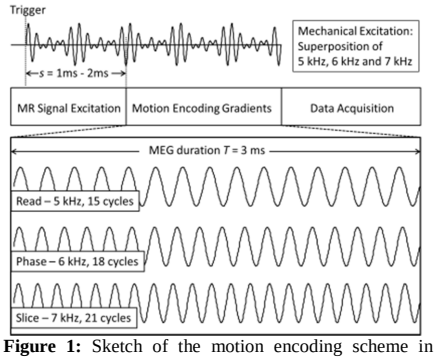

Figure 1: Sketch of the motion encoding scheme in SDP-MRE is shown during one TR. All three MEGs were applied simultaneously. The trigger was shifted 16 times over the 1 ms interval for temporal resolution. See text for more details.

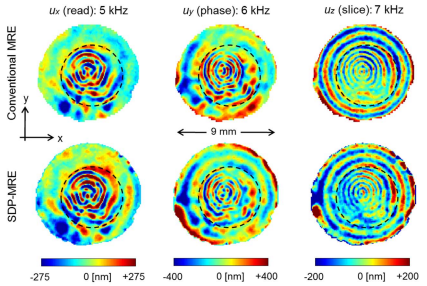

Figure 2: Complex wave images (real part) are shown for the axial image slice. The agarose bead inside the agarose gel is demarcated with dashed lines. The three images in the top row correspond to conventional MRE experiments conducted in individual, consecutive steps. Images in the bottom row were acquired simultaneously with SDP-MRE. Motion encoding direction for the 5 kHz-, 6 kHz- and 7 kHz-vibration was read, phase and slice, respectively.

Results: The complex wave images acquired with SDP-MRE and with conventional MRE are illustrated in fig. 2. The wavelength λ varies from column to column, as both, the vibration frequency and the displacement projection changes. For the same reason we also observe different wave amplitudes in different projections using the same method. There is a less pronounced difference in wave amplitude visible in the same projection measured with each of the two methods, but no systematic variation is evident. More importantly, we observe similar wave structures for same projections in figure 2. Consequently, the LFE-derived wavelengths are identical within the error margins. The spatial average of λ over the agarose bead results in (0.7±0.1) mm, (0.5±0.1) mm and (0.4±0.1) mm for the 5 kHz-, 6 kHz- and 7 kHz-vibration, respectively, independently of the used MRE approach.

Discussion and Conclusion: In the presented proof-of-concept study, SDP-MRE was successfully applied to a 3D multifrequency vibration. We selected the 5 kHz-, 6 kHz- and 7 kHz-frequency for the read-, phase- and slice-projection of the displacement, respectively, and acquired these components simultaneously within one temporally-resolved MRE experiment. For the acquisition of the full 3D-three frequency vibration spectrum, these relations are permuted resulting in only three SDP-MRE experiments. Thus, SDP-MRE enables a reduction in the necessary number of individual MRE experiments from nine to three in comparison with conventional MRE, while the LFE-derived wavelengths are identical within the error margins. As a concept for the 3D arrangement of the MEG, SDP-MRE is not bound to a specific sequence type, but can be integrated in most pulse sequences typically used in MRE, such as gradient-echo, spin-echo and EPI.

References: [1] Muthupillai et al., Science 269, 1854-1857 (1995); [2] Klatt et al., Phys Med Biol 52, 7281-7294 (2007); [3] Freimann et al., Neuroradiology 54, 189-196 (2012); [4] Asbach et al., Radiology 257, 80-86 (2010); [5] Sinkus et al., Magn Reson Imaging 23, 159-165 (2005); [6] Hirsch et al., MRM, doi: 10.1002/mrm.24499 (online); [7] Rump et al., MRM 57, 388-395 (2007); [8] Sack et al., MRM 52, 842-850 (2004); [9] Yasar et al., MRM, doi: 10.1002/mrm.24495 (online); [10] Knutsson et al., Proc IEEE ICIP-94, 36-40 (1994). **Acknowledgement**: NIH support EB007537, EB012142.